Complementarity of the constraints on new physics from $B_s \to \mu^+\mu^-$ and from $B \to K\ell^+\ell^-$ decays

Damir Bečirević,[1] Nejc Košnik,[2] Federico Mescia,[3] and Elia Schneider[4]

[1]*Laboratoire de Physique Théorique (Bâtiment 210)*Université Paris Sud, Centre d'Orsay, F-91405 Orsay Cedex, France*
[2]*Laboratoire de l'Accélérateur Linéaire, Centre d'Orsay, Université de Paris-Sud XI, B.P. 34, Bâtiment 200, 91898 Orsay Cedex, France, and J. Stefan Institute, Jamova 39, P. O. Box 3000, 1001 Ljubljana, Slovenia*
[3]*Departament d'Estructura i Constituents de la Matèria and Institut de Ciències del Cosmos (ICCUB), Universitat de Barcelona, 08028 Barcelona, Spain*
[4]*Dipartimento di Fisica, Università degli Studi di Trento, and INFN Gruppo collegato di Trento Via Sommarive 14, Povo (Trento) I-38123, Italy*

We discuss the advantages of combining the experimental bound on Br($B_s \to \mu^+\mu^-$) and the measured Br($B \to K\ell^+\ell^-$) to get the model-independent constraints on physics beyond the Standard Model. Since the two decays give complementary information, one can study not only the absolute values of the Wilson coefficients that are zero in the Standard Model, but also their phases. To identify the sector in which the new physics might appear, information about the shapes of the transverse asymmetries in $B \to K^*\ell^+\ell^-$ at low q^2's can be particularly useful. We also emphasize the importance of measuring the forward-backward asymmetry in $B \to K\ell^+\ell^-$ decay at large q^2's.

PACS numbers: 13.20.He, 12.60.−i

I. INTRODUCTION AND BASIC FORMULAS

Ever since the first observation of $B \to K^*\gamma$ [1], the decay modes governed by the loop-induced $b \to s$ transition have played a major role in the search for signals of physics beyond the Standard Model (BSM) in low-energy experiments. After years of experimental and theoretical effort, we now know that the observed decay rates and several conveniently defined observables are consistent with the Standard Model (SM) predictions, thus leaving little room for new physics (NP). Since the nonperturbative QCD (hadronic) uncertainties are still large in most cases, the comparison between theory and experiment is not yet at the precision level, and quantitative statements about the size of possible NP contributions are often subjects of controversy.

Much of the experimental activity has been devoted to $B \to K^*\ell^+\ell^-$ decay, for which improvement on theoretical (hadronic) uncertainties is hard to achieve, apart from a few asymmetries that will be studied at CMS, LHCb and in the new generation of B-physics experiments. In contrast to the decay to K^*, a substantial improvement in the determination of the hadronic form factors entering the theoretical description of $B \to K\ell^+\ell^-$ is realistic to expect very soon. In that respect, the recently reported result on Br($B \to K\ell^+\ell^-$) by *BABAR* [2] is likely to become a major constraint in the NP searches. The ongoing experimental effort to detect another $b \to s$ mediated decay, $B_s \to \mu^+\mu^-$, has been greatly improved after LHCb was able to set an upper bound on Br($B_s \to \mu^+\mu^-$) that got very close to the value predicted in the SM [3]. In this paper we

discuss how these two decay modes can be combined to give us complementary information about the potential physics contributions from BSM.

The most important effect of physics BSM in $B_s \to \mu^+\mu^-$ is expected to come from a coupling to the scalar and/or the pseudoscalar operators. If that scenario is verified in nature, it would strongly affect $B \to K\ell^+\ell^-$, whereas the three transverse asymmetries $A_T^{(2,\mathrm{im,re})}(q^2)$ of $B \to K^*\ell^+\ell^-$ decay would remain unchanged with respect to their shapes predicted at low q^2's in the SM [4].[1] If, instead, the NP alters the couplings to the semileptonic operators $\propto \bar{s}\gamma_\mu P_{L,R} b$, then the shapes of the mentioned asymmetries would change too.

In this paper we assume that the NP does not couple with tensor operators (specified below). It turns out that this assumption can also be tested by measuring $A_{FB}^\ell(q^2)$, the forward-backward asymmetry in $B \to K\ell^+\ell^-$, but in the region of large q^2's in which the nonzero tensor couplings would entail a large enhancement of $A_{FB}^\ell(q^2)$.

In what follows, we will show how and why the two decay modes, $B_s \to \mu^+\mu^-$ and $B \to K\ell^+\ell^-$, are complementary, and after combining the recent experimental results with our current theoretical knowledge of the hadronic matrix elements, we will discuss the resulting constraints on NP.

In handling the $B \to K\ell^+\ell^-$ decay we computed the form factors by using the simulations of quenched QCD on the lattice (LQCD), which appear to be compatible with the results obtained by evaluating the QCD sum rules near the light cone (LCSR) [6]. These results are merely an

---

[1]Please note that the asymmetry $A_T^{(2)}(q^2)$ has been introduced in Ref. [5] and since then abundantly discussed in the literature.

illustration of the potential of LQCD in pinning down the hadronic errors in this decay. Very soon these results will be substantially improved by using the available QCD configurations that contain the effects of dynamical quarks [7]. Notice that the lattice results are more reliable in the larger half of the q^2 region available from this decay ($14 \text{ GeV}^2 \lesssim q^2 \lesssim 20 \text{ GeV}^2$). For that reason it would be desirable to have the experimentally established partial decay width of $B \to K \ell^+ \ell^-$ at q^2's that are also accessible in modern lattice QCD studies. In that way we would be far more confident about the quantitative statements made from this kind of analysis.

The effective Hamiltonian describing the $b \to s \ell^+ \ell^-$ transitions at low energy is [8]

$$\mathcal{H}_{\text{eff}} = -\frac{4G_F}{\sqrt{2}} V_{tb} V_{ts}^* \left[\sum_{i=1}^{6} C_i(\mu) \mathcal{O}_i(\mu) \right.$$
$$\left. + \sum_{i=7,8,9,10,P,S,T,T5} (C_i(\mu) \mathcal{O}_i + C_i'(\mu) \mathcal{O}_i') \right], \quad (1)$$

where the twice Cabibbo-suppressed contributions ($\propto V_{ub} V_{us}^*$) have been neglected. The operator basis in which the Wilson coefficients have been computed is [9,10]

$$\mathcal{O}_7 = \frac{e}{g^2} m_b (\bar{s} \sigma_{\mu\nu} P_R b) F^{\mu\nu}, \qquad \mathcal{O}_7' = \frac{e}{g^2} m_b (\bar{s} \sigma_{\mu\nu} P_L b) F^{\mu\nu}, \qquad \mathcal{O}_8 = \frac{1}{g} m_b (\bar{s} \sigma_{\mu\nu} T^a P_R b) G^{\mu\nu a},$$

$$\mathcal{O}_8' = \frac{1}{g} m_b (\bar{s} \sigma_{\mu\nu} T^a P_L b) G^{\mu\nu a}, \qquad \mathcal{O}_9 = \frac{e^2}{g^2} (\bar{s} \gamma_\mu P_L b)(\bar{\ell} \gamma^\mu \ell), \qquad \mathcal{O}_9' = \frac{e^2}{g^2} (\bar{s} \gamma_\mu P_R b)(\bar{\ell} \gamma^\mu \ell),$$

$$\mathcal{O}_{10} = \frac{e^2}{g^2} (\bar{s} \gamma_\mu P_L b)(\bar{\ell} \gamma^\mu \gamma_5 \ell), \qquad \mathcal{O}_{10}' = \frac{e^2}{g^2} (\bar{s} \gamma_\mu P_R b)(\bar{\ell} \gamma^\mu \gamma_5 \ell), \qquad \mathcal{O}_S = \frac{e^2}{16\pi^2} (\bar{s} P_R b)(\bar{\ell} \ell), \quad (2)$$

$$\mathcal{O}_S' = \frac{e^2}{16\pi^2} (\bar{s} P_L b)(\bar{\ell} \ell), \qquad \mathcal{O}_P = \frac{e^2}{16\pi^2} (\bar{s} P_R b)(\bar{\ell} \gamma_5 \ell), \qquad \mathcal{O}_P' = \frac{e^2}{16\pi^2} (\bar{s} P_L b)(\bar{\ell} \gamma_5 \ell),$$

$$\mathcal{O}_T = \frac{e^2}{16\pi^2} (\bar{s} \sigma_{\mu\nu} b)(\bar{\ell} \sigma^{\mu\nu} \ell), \qquad \mathcal{O}_{T5} = \frac{e^2}{16\pi^2} (\bar{s} \sigma_{\mu\nu} b)(\bar{\ell} \sigma^{\mu\nu} \gamma_5 \ell),$$

where $P_{L,R} = (1 \mp \gamma_5)/2$, $\ell = e$ or μ, and the explicit expressions for $\mathcal{O}_{1-6}$ can be found in Ref. [9]. Short-distance physics effects, encoded in the Wilson coefficients $C_i(\mu)$, have been computed in the SM through a perturbative matching of the effective with the full theory at $\mu = m_W$, and then evolved down to $\mu = m_b$ by means of the QCD renormalization group equations at next-to-next-to-leading logarithmic approximation [9]. It is customary to reassemble Wilson coefficients multiplying the same hadronic matrix element into effective coefficients appearing in the physical amplitudes, namely [11]

$$C_7^{\text{eff}} = \frac{4\pi}{\alpha_s} C_7 - \frac{1}{3} C_3 - \frac{4}{9} C_4 - \frac{20}{3} C_5 - \frac{80}{9} C_6,$$

$$C_8^{\text{eff}} = \frac{4\pi}{\alpha_s} C_8 + C_3 - \frac{1}{6} C_4 + 20 C_5 - \frac{10}{3} C_6,$$

$$C_9^{\text{eff}} = \frac{4\pi}{\alpha_s} C_9 + Y(q^2), \qquad C_{10}^{\text{eff}} = \frac{4\pi}{\alpha_s} C_{10}, \quad (3)$$

$$C_{7,8,9,10}'^{\text{,eff}} = \frac{4\pi}{\alpha_s} C_{7,8,9,10}',$$

where the function $Y(q^2)$ is

$$Y(q^2) = \frac{4}{3} C_3 + \frac{64}{9} C_5 + \frac{64}{27} C_6 - \frac{1}{2} h(q^2,0)\left(C_3 + \frac{4}{3} C_4 + 16 C_5 \right.$$
$$\left. + \frac{64}{3} C_6 \right) + h(q^2, m_c)\left(\frac{4}{3} C_1 + C_2 + 6 C_3 + 60 C_5\right)$$
$$- \frac{1}{2} h(q^2, m_b)\left(7 C_3 + \frac{4}{3} C_4 + 76 C_5 + \frac{64}{3} C_6\right), \quad (4)$$

and

$$h(q^2, m_q) = -\frac{4}{9}\left(\ln\frac{m_q^2}{\mu^2} - \frac{2}{3} - z\right) - \frac{4}{9}(2 + z)\sqrt{|z-1|}$$
$$\times \begin{cases} \arctan\frac{1}{\sqrt{z-1}} & z > 1 \\ \ln\frac{1+\sqrt{1-z}}{\sqrt{z}} - \frac{i\pi}{2} & z \leq 1 \end{cases}, \quad (5)$$

with $z = 4m_q^2/q^2$. To make the notation less heavy, in what follows we will drop the superscript "eff" in Wilson coefficients, while tacitly assuming the redefinitions in Eq. (3). Note that in the SM the Wilson coefficients of the right-handed flavor violating operators or of the operators $\mathcal{O}_{S,P,T,T5}$ are absent and therefore $C_{7,8,9,10}' = C_{S,P,T,T5}^{(\prime)} = 0$.

II. PHYSICAL PROCESSES AS CONSTRAINTS

A. $B_s \to \ell^+ \ell^-$

One of the most promising decay modes expected to reveal the effects of NP at LHCb is $B_s \to \mu^+ \mu^-$. Using the effective theory [Eq. (1)], the only operator contributing to the amplitude of this process in the SM is $\mathcal{O}_{10}$, and the expression for the branching fraction of this decay reads

$$\text{Br}(B_s \to \ell^+ \ell^-)^{\text{SM}}$$
$$= \tau_{B_s} \frac{G_F^2 \alpha^2}{16\pi^3} |V_{tb} V_{ts}^*|^2 m_{B_s} m_\ell^2 \beta_\ell(m_{B_s}^2) |C_{10}|^2 f_{B_s}^2, \quad (6)$$

where $\beta_\ell(q^2) = \sqrt{1 - 4m_\ell^2/q^2}$, $\ell = \mu$ or e, and the B_s meson decay constant is defined via

$$\langle 0|\bar{s}\gamma_\mu P_L b|B_s(p)\rangle = \frac{i}{2} f_{B_s} p_\mu. \tag{7}$$

On general grounds, the contributions of physics beyond the SM can modify the above expression to

$$\mathrm{Br}(B_s \to \ell^+\ell^-)^{\mathrm{BSM}} = \tau_{B_s} f_{B_s}^2 m_{B_s}^3 \frac{G_F^2 \alpha^2}{64\pi^3} |V_{tb}V_{ts}^*|^2 \beta_\ell(m_{B_s}^2)$$
$$\times \left[\frac{m_{B_s}^2}{m_b^2}|C_S - C_S'|^2\left(1 - \frac{4m_\ell^2}{m_{B_s}^2}\right) \right.$$
$$+ \left| \frac{m_{B_s}}{m_b}(C_P - C_P') \right.$$
$$\left. \left. + 2\frac{m_\ell}{m_{B_s}}(C_{10} - C_{10}') \right|^2 \right], \tag{8}$$

thus lifting the helicity suppression exhibited in the SM expression [Eq. (6)]. This is why it is interesting and important to experimentally investigate this decay for both $\ell = \mu$ and $\ell = e$. In the SM, the electron mass severely suppresses the decay rate, and a clean detection of the $B_s \to e^+e^-$ events would be a clear signal of NP effects. In the last formula the presence of the right-handed (non-SM) couplings would induce $C_{10}' \neq 0$, while the new scalar (pseudoscalar) couplings would entail the nonzero $C_S^{(\prime)}$ ($C_P^{(\prime)}$).

Several specific NP models that allow for large values of C_S suggested a possibility of observing a large number of $B_s \to \mu^+\mu^-$ events. Recent experimental activity at the LHC [3], however, showed that such a large enhancement does not occur and the current upper bound on $\mathrm{Br}(B_s \to \mu^+\mu^-)$ is quite close to the SM value. More specifically,[2]

$$\mathrm{Br}(B_s \to \mu^+\mu^-)^{\mathrm{exp}} < 4.1 \times 10^{-9},$$
$$\mathrm{Br}(B_s \to \mu^+\mu^-)^{\mathrm{th\text{-}SM}} = (3.3 \pm 0.3) \times 10^{-9}, \tag{9}$$

where for the SM estimate we used the parameters given in Appendix B of the present paper (cf., Table II). Although the desired enhancement by orders of magnitude with respect to the SM does not occur, the possibility of seeing the NP signal from this decay mode is still alive. One can even envisage the possibility of $\mathrm{Br}(B_s \to \mu^+\mu^-)$ smaller than the one predicted in the SM, as can be easily seen from Eq. (8).

---

[2]Recently, it has been noted that the effect of $B_s - \bar{B}_s$ mixing should be taken into account [12], whose net effect amounts to replacing $\mathrm{Br}(B_s \to \mu^+\mu^-)^{\mathrm{exp}} \to (1 - y_s)\,\mathrm{Br}(B_s \to \mu^+\mu^-)^{\mathrm{exp}}$, where $y_s = (\Delta\Gamma/2\Gamma)_{B_s} = (9.0 \pm 2.1 \pm 0.8)\%$ was also measured by LHCb [13]. This correction is already incorporated in the corrected experimental value [Eq. (10)].
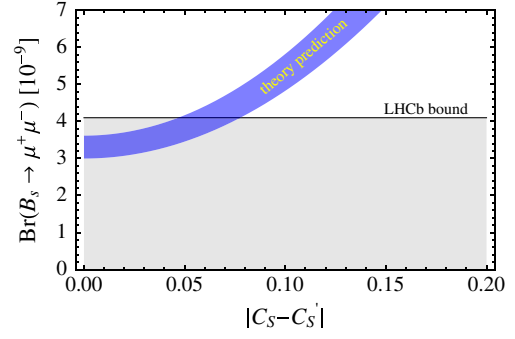

FIG. 1 (color online). Increase of $\mathrm{Br}(B_s \to \mu^+\mu^-)$ with $|C_S - C_S'|$ according to Eq. (8) is shown by the dark band, defined by 1σ errors on the input parameters. The brightly shaded area depicts the experimentally allowed values for the decay mode. $C_{10}' = C_P^{(\prime)} = 0$ has been used.

If, for the moment, we only consider the possibility that the SM is extended by allowing a coupling to the scalar operator, i.e., by keeping $C_{10}' = C_P^{(\prime)} = 0$, then from Eq. (8) one gets

$$|C_S - C_S'| \leq 0.08 \qquad (1\sigma), \tag{10}$$

which we illustrate in Fig. 1. This limit is actually not too far away from $|C_S - C_S'|^{\mathrm{SM}} = 0$, which is why this bound becomes a very severe constraint on the NP models with scalar operators. The above bound still allows for an observation of $\mathrm{Br}(B_s \to e^+e^-) \lesssim 2 \times 10^{-9}$, unless the lepton flavor universality is not respected by NP. Obviously, the bound in Eq. (10) does not give us any information about C_S and C_S' separately. For that we would need the complementary information that can be inferred from $B \to K\ell^+\ell^-$.

Recent research about exploring the constraint from the experimental bound on $\mathrm{Br}(B_s \to \mu^+\mu^-)$ has been reported in Ref. [19].

B. $B \to K\ell^+\ell^-$

There are many papers in the literature dealing with this decay. We were able to check the expressions given in Ref. [20] with which we agree. The full distribution of this decay is conveniently expressed as

$$\frac{d^2\Gamma_\ell(q^2, \cos\theta)}{dq^2 d\cos\theta} = a_\ell(q^2) + b_\ell(q^2)\cos\theta + c_\ell(q^2)\cos^2\theta, \tag{11}$$

where for short $\Gamma_\ell \equiv \Gamma(B \to K\ell^+\ell^-)$, $q^2 = (p_{\ell^+} + p_{\ell^-})^2$, and θ is the angle between the directions of $\bar{B}$ and of ℓ^- in the center-of-mass frame of the lepton pair. In terms of specific Lorentz components, $F_i(q^2)$ ($i = S, P, V, A, T, T5$), the explicit expressions of the functions on the right hand side of Eq. (13) are

$$a_\ell(q^2) = \mathcal{C}(q^2)\Bigg[q^2(\beta_\ell^2(q^2)|F_S(q^2)|^2 + |F_P(q^2)|^2) + \frac{\lambda(q^2)}{4}(|F_A(q^2)|^2 + |F_V(q^2)|^2) + 4m_\ell^2 m_B^2 |F_A(q^2)|^2$$

$$+ 2m_\ell(m_B^2 - m_K^2 + q^2)\,\mathrm{Re}(F_P(q^2)F_A^*(q^2))\Bigg],$$

$$b_\ell(q^2) = 2\mathcal{C}(q^2)\{q^2[\beta_\ell^2(q^2)\,\mathrm{Re}(F_S(q^2)F_T^*(q^2)) + \mathrm{Re}(F_P(q^2)F_{T5}^*(q^2))] + m_\ell[\sqrt{\lambda(q^2)}\beta_\ell(q^2)\,\mathrm{Re}(F_S(q^2)F_V^*(q^2))$$

$$+ (m_B^2 - m_K^2 + q^2)\,\mathrm{Re}(F_{T5}(q^2)F_A^*(q^2))]\},$$

$$c_\ell(q^2) = \mathcal{C}(q^2)\Bigg[q^2(\beta_\ell^2(q^2)|F_T(q^2)|^2 + |F_{T5}(q^2)|^2) - \frac{\lambda(q^2)}{4}\beta_\ell^2(q^2)(|F_A(q^2)|^2 + |F_V(q^2)|^2)$$

$$+ 2m_\ell\sqrt{\lambda(q^2)}\beta_\ell(q^2)\,\mathrm{Re}(F_T(q^2)F_V^*(q^2))\Bigg], \tag{12}$$

where

$$\mathcal{C}(q^2) = \frac{G_F^2 \alpha^2 |V_{tb}V_{ts}^*|^2}{512\pi^5 m_B^3}\beta_\ell(q^2)\sqrt{\lambda(q^2)}, \tag{13}$$

with

$$\lambda(q^2) = q^4 + m_B^4 + m_K^4 - 2(m_B^2 m_K^2 + m_B^2 q^2 + m_K^2 q^2) \tag{14}$$

and

$$F_V(q^2) = (C_9 + C_9')f_+(q^2) + \frac{2m_b}{m_B + m_K}$$

$$\times \left(C_7 + C_7' + \frac{4m_\ell}{m_b}C_T\right)f_T(q^2),$$

$$F_A(q^2) = (C_{10} + C_{10}')f_+(q^2),$$

$$F_S(q^2) = \frac{m_B^2 - m_K^2}{2m_b}(C_S + C_S')f_0(q^2),$$

$$F_P(q^2) = \frac{m_B^2 - m_K^2}{2m_b}(C_P + C_P')f_0(q^2) - m_\ell(C_{10} + C_{10}')$$

$$\times \left[f_+(q^2) - \frac{m_B^2 - m_K^2}{q^2}(f_0(q^2) - f_+(q^2))\right],$$

$$F_T(q^2) = \frac{2\sqrt{\lambda(q^2)}\beta_\ell(q^2)}{m_B + m_K}C_T f_T(q^2),$$

$$F_{T5}(q^2) = \frac{2\sqrt{\lambda(q^2)}\beta_\ell(q^2)}{m_B + m_K}C_{T5} f_T(q^2). \tag{15}$$

In the above expressions we employed the standard decompositions of the hadronic matrix elements in terms of the form factors, namely

$$\langle K(k)|\bar{s}\gamma_\mu b|B(p)\rangle = \left[(p+k)_\mu - \frac{m_B^2 - m_K^2}{q^2}q_\mu\right]f_+(q^2)$$

$$+ \frac{m_B^2 - m_K^2}{q^2}q_\mu f_0(q^2),$$

$$\langle K(k)|\bar{s}\sigma_{\mu\nu} b|B(p)\rangle = -i(p_\mu k_\nu - p_\nu k_\mu)\frac{2f_T(q^2)}{m_B + m_K}. \tag{16}$$

After integrating Eq. (11) over $q^2 = (p - k)^2$, one obtains

$$\frac{d\Gamma_\ell(\cos\theta)}{d\cos\theta} = A_\ell + B_\ell\cos\theta + C_\ell\cos^2\theta, \tag{17}$$

where obviously

$$A_\ell = \int_{q_{\min}^2}^{q_{\max}^2} a_\ell(q^2)dq^2, \qquad B_\ell = \int_{q_{\min}^2}^{q_{\max}^2} b_\ell(q^2)dq^2,$$

$$C_\ell = \int_{q_{\min}^2}^{q_{\max}^2} c_\ell(q^2)dq^2, \tag{18}$$

with $q_{\min}^2 = 4m_\ell^2$, and $q_{\max}^2 = (m_B - m_K)^2$. For a partial decay width, one would obviously choose different $q_{\min/\max}^2$. Finally, the integration over θ leads to the full decay width, in which the term proportional to $\cos\theta$ drops out. The latter survives in the forward-backward asymmetry, and we have

$$\Gamma_\ell = 2\left(A_\ell + \frac{1}{3}C_\ell\right), \qquad A_{FB}^\ell = \frac{B_\ell}{\Gamma_\ell}. \tag{19}$$

Clearly these two observables are independent, as they involve different pieces of the distribution [Eq. (11)]. In Ref. [20] another useful quantity has been introduced,

$$F_H^\ell = \frac{2(A_\ell + C_\ell)}{\Gamma_\ell}, \tag{20}$$

which in the SM is proportional to m_ℓ^2, but can receive important contributions in various scenarios of NP. Before continuing, we wish to stress that in the SM $A_{FB}^\ell = 0$, and it remains zero even if the Wilson coefficients $C_{7,9,10}^{(l)}$ received large NP contributions. Its nonzero measurement would be a clean signal of NP, and therefore its experimental study would be highly welcome.

For our purpose, it is important to note that all the functions in Eqs. (12) and (15) involve the sum of $C_i + C_i'$, and therefore the full branching ratio provides us with a constraint that is complementary to Eq. (10). The recently measured [2]

$$\mathrm{Br}\,(B \to K\ell^+\ell^-)_{\exp} = (4.7 \pm 0.6 \pm 0.2) \times 10^{-7} \tag{21}$$

is compatible with the SM prediction,

$$\mathrm{Br}(B \to K\ell^+\ell^-)_{\mathrm{SM}} = \begin{cases} (7.5 \pm 1.4) \times 10^{-7} & \mathrm{LQCD} \\ (6.8 \pm 1.6) \times 10^{-7} & \mathrm{LCSR} \end{cases}, \quad (22)$$

which, at this stage, we take to be

$$\mathrm{Br}(B \to K\ell^+\ell^-)_{\mathrm{SM}} = (7.0 \pm 1.8) \times 10^{-7}, \quad (23)$$

thus covering all the values allowed by the two methods of computing the form factors, LQCD and LCSR. Allowing for nonzero $C_S^{(l)}$ then leads to

$$|C_S + C_S'| \le 1.3 \qquad (1\sigma), \quad (24)$$

as illustrated in Fig. 2. To obtain Eq. (24), we had to assume that NP does not alter the SM values of $C_{7,9}^{(l)}$ which enter the expression for $\mathrm{Br}(B \to K\ell^+\ell^-)$. That assumption can be tested experimentally through the study of low-q^2 behavior of three transverse asymmetries discussed in Ref. [4] which exhibit three very important features: (i) they have small hadronic uncertainties, (ii) their shapes are highly sensitive to $C_{7,9}^{(l)}$, and (iii) they are completely insensitive to $C_{S,P}^{(l)}$.

Another important comment concerning the constraint in Eq. (24) is that it is obtained by including the 1σ experimental uncertainty, and by using the form factors that are either obtained from the numerical simulations of quenched QCD on the lattice (see Appendix B of this paper) or in the QCD sum rule analyzed near the light cone [6], respectively labeled as LQCD and LCSR in Eq. (22). LQCD results appear to be consistent with those obtained from LCSR. The three relevant form factors, $f_{+,0,T}(q^2)$, will soon be improved by the new generation of unquenched lattice QCD simulations. Several such studies are underway [7]. Notice that the improvement of $f_{+,0,T}(q^2)$ is much more realistic to expect than those parameterizing the $B \to K^*$ transition matrix elements, because the latter decay involves many more form factors, including at least three that suffer from very large uncertainties (see e.g., Ref. [21]).
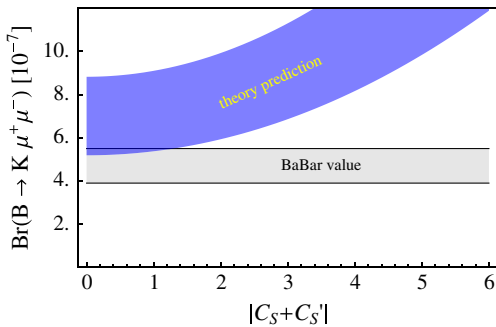

FIG. 2 (color online). $\mathrm{Br}(B \to K\ell^+\ell^-) = \tau_B \Gamma_\ell$ as a function of $|C_S + C_S'|$. Bright shaded horizontal band corresponds to the recently measured $\mathrm{Br}(B \to K\ell^+\ell^-)$ at *BABAR*. We used Γ_ℓ given in Eq. (19) and $\tau_B = \tau_{B^0}$ to conform with the experimental practice when combining neutral and charged B modes.

III. CONSTRAINTS ON THE SCALAR (PSEUDOSCALAR) COUPLINGS

Couplings to the scalar and pseudoscalar operators are particularly interesting in the framework of supersymmetric (SUSY) extensions of the SM. A very detailed consideration of the SUSY contributions to $B_s \to \ell^+\ell^-$ has been made in Ref. [22]. The relations between the Wilson coefficients $C_{S,P}^{(l)}$ and $C_{LL,LR,RL,RR}^S$, defined in Ref. [22] are

$$\begin{aligned} C_S &= X(C_{LR}^S + C_{LL}^S)^*, & C_P &= X(C_{LR}^S - C_{LL}^S)^*, \\ C_S' &= X(C_{RR}^S + C_{RL}^S)^*, & C_P' &= X(C_{RR}^S - C_{RL}^S)^*, \end{aligned} \quad (25)$$

where $X = \pi/(\sqrt{2}G_F \alpha V_{ts}^* V_{tb})$. From Ref. [22] we learn that the SUSY contributions to the box and penguin diagrams can modify $C_{S,P}^{(l)}$ as follows:

(i) Diagrams with one charged Higgs boson propagating in the box can give a nonzero contribution via coupling to the left-handed parts only. Furthermore, they verify $C_S^{H^+} = -C_P^{H^+}$. The right-handed couplings, instead, are suppressed by the strange quark mass, $C_S'^{H^+} = C_P'^{H^+} = 0$.

(ii) Diagrams with charginos propagating in the box also give rise to C_S^χ and C_P^χ, but leave $C_S'^\chi = C_P'^\chi = 0$. Moreover, if for example the masses of squarks and sneutrinos in the box are degenerate, then one again obtains $C_S^\chi = -C_P^\chi$.

(iii) The Z^0-penguin diagram, with superparticles propagating in the loop, cannot generate a contribution to $C_{S,P}^{(l)}$ due to the vector coupling to Z^0.

(iv) The H^0-penguin diagram, instead, can give a sizable contribution, which verifies

$$C_S^{H^0} = -C_P^{H^0}, \qquad C_S'^{H^0} = C_P'^{H^0} \quad (26)$$

up to the electroweak symmetry-breaking corrections that are proportional to the mass splitting between the SUSY (MSSM) Higgs bosons, namely $m_{H^0}^2 - m_{A^0}^2$.

The situation similar to the H^0-penguin case above also happens in the models with vector leptoquark states. In those models, nonzero contributions to C_S are possible, and they satisfy the relation $C_S = \pm C_P$, as well as $C_S' = \mp C_P'$ [23]. On the contrary, the models with scalar leptoquarks cannot generate any sizeable value of $C_{S,P}^{(l)}$. These are obviously only two among many scenarios of physics BSM in which the coupling to scalar (pseudoscalar) can be generated.

In the remainder of this section we will combine the constraints discussed in Sec. II and apply them to two particular scenarios: (1) $C_S^{(l)} \ne 0$, while $C_{10}' = C_P^{(l)} = 0$, and (2) $C_P^{(l)} \ne 0$, while keeping $C_{10}' = C_S^{(l)} = 0$. In each case we will also allow the nonzero relative phase between the left- and right-handed couplings (Wilson coefficients).
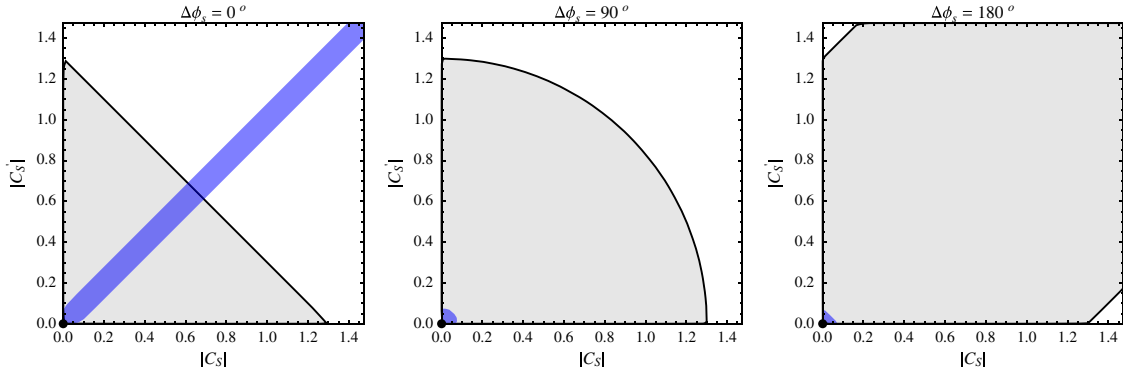
FIG. 3 (color online). The constraint on $|C_S|$ and $|C_S'|$ obtained from Br($B \to K\ell^+\ell^-$) is represented by the brightly shaded area, whereas the one deduced from Br($B_s \to \mu^+\mu^-$) is described by the dark shaded region. Of course, only the overlap of both regions is consistent with the constraints. It is also consistent with Br($B \to X_s\ell^+\ell^-$) and $|C_S^{(\prime)}| \neq 0$; it does not modify the transverse asymmetries in $B \to K^*\ell^+\ell^-$. Plotted are the cases with three specific choices of the relative phase $\Delta\phi_S$.

A. $C_S^{(\prime)} \neq 0$

We first focus on the scenario in which C_S and C_S' can be different from zero. Besides $|C_S^{(\prime)}| \neq 0$, NP can induce new weak phases, which through our constraints in Eqs. (10) and (24) cannot be studied separately. Instead, one can study the impact of the relative phase, $\Delta\phi_S = \phi_S' - \phi_S$, by using

$$|C_S \pm C_S'|^2 = |C_S|^2 + |C_S'|^2 \pm 2|C_S||C_S'|\cos(\Delta\phi_S) \quad (27)$$

and explore the possible values of $|C_S|$ and $|C_S'|$ for various $\Delta\phi_S \in [0, \pi]$ that are compatible with the constraints in Eqs. (10) and (24). The bound on $B_s \to \mu^+\mu^-$ is much more compelling, and for any nonzero relative phase, $\Delta\phi_S$, the constraint provided by $B \to K\ell^+\ell^-$ becomes essentially superfluous, except in the case of $\Delta\phi_S = 0$ when the constraint of Eq. (10) describes a stripe in the plane ($|C_S|$, $|C_S'|$) that is cut off by the constraint of Eq. (24). This situation is illustrated in Fig. 3 for three representative cases, $\Delta\phi_S = 0$, $\pi/2$, and π. We see that the situation in which $\Delta\phi_S = 0$ is indeed peculiar, and only for very small values of the relative phase $\Delta\phi_S$ are the sizable couplings to NP via scalar operators possible. Otherwise a nonzero relative phase entails a reduction of available $|C_S^{(\prime)}|$, as we show in Fig. 4. Two important comments are in order:

(i) Any value of $|C_S|$ and/or $|C_S'|$ allowed by the constraints in Eqs. (10) and (24), for any value of the relative phase $\Delta\phi_S$, is consistent with the branching fraction of the inclusive $B \to X_s\ell^+\ell^-$ decay, which has been measured at the B factories at low q^2's [24,25], resulting in an average [26],

$$\int_{1\,\text{GeV}^2}^{6\,\text{GeV}^2} \frac{d\text{Br}(B \to X_s\mu^+\mu^-)}{dq^2} dq^2|_{\text{exp}} = 1.6(5) \times 10^{-6}.$$

$$(28)$$

By using the formulas presented in Refs. [26,27], we obtain in the SM

$$\int_{1\,\text{GeV}^2}^{6\,\text{GeV}^2} \frac{d\text{Br}(B \to X_s\mu^+\mu^-)}{dq^2} dq^2|_{\text{th-SM}}$$
$$= 1.59(17) \times 10^{-6}, \quad (29)$$

where, instead of the usual practice to normalize by the inclusive semileptonic $\Gamma(B \to X_c e\nu)$ decay, we actually use the tree-level decay rate proportional to the fifth power of the b-quark mass, i.e.,

$$B_0 = \tau_B \frac{4\alpha^2 G_F^2 |V_{tb} V_{ts}^*|^2 m_b^5}{3(4\pi)^5} = 3.41(47) \times 10^{-7}, \quad (30)$$

which is now possible thanks to the fact that the value of the b-quark is by now very well determined from the multitude of techniques of QCD sum rules and modern simulations of QCD on the lattice. Our result agrees very well with the one obtained in Ref. [26] that was obtained by normalizing to $\Gamma(B \to X_c e\nu)$. In practice we take the average quark mass quoted by PDG and convert it to the pole mass using the next-to-next-to-leading logarithmic approximation perturbative QCD corrections [28].
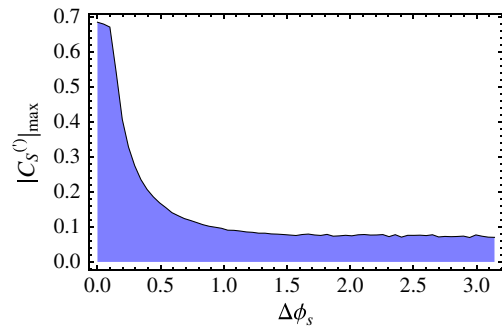

FIG. 4 (color online). Maximal value of $|C_S|$ or $|C_S'|$ allowed by the constraints in Eqs. (10) and (24) as a function of the relative phase $\Delta\phi_S \in [0, \pi]$.
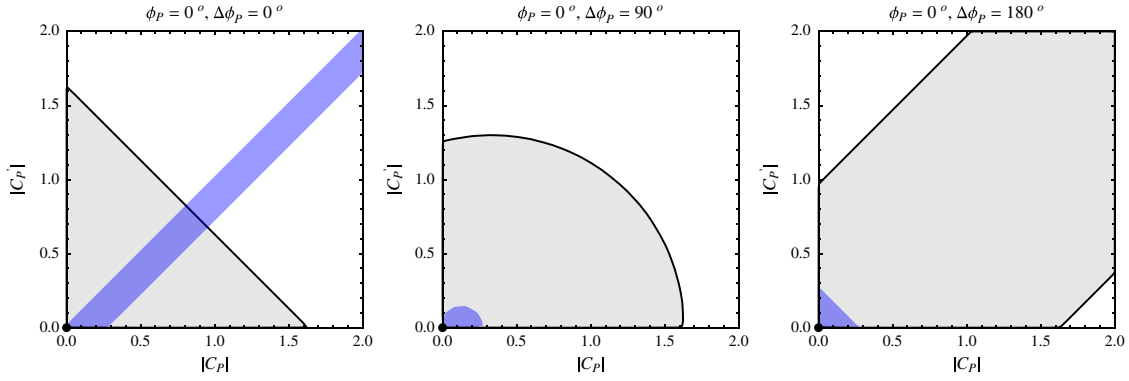
FIG. 5 (color online). Allowed values for $|C_P|$ and $|C'_P|$ correspond to the overlap of the constraints obtained from $\mathrm{Br}(B \to K\ell^+\ell^-)$ (light shaded area) and $\mathrm{Br}(B_s \to \mu^+\mu^-)$ (dark shaded area). Illustration is provided for three various values of the relative phase $\Delta\phi_P$ and for $\phi_P = 0$.

The scalar contribution to $B \to X_s\mu^+\mu^-$ has been computed in Ref. [29], and leads to a term that adds up to $\mathrm{Br}(B \to X_s\ell^+\ell^-)_{\mathrm{SM}}$ and reads

$$\frac{d\mathrm{Br}(B \to X_s\mu^+\mu^-)}{dq^2}\bigg|_{C_S^{(l)}} = \frac{3B_0}{2m_b^2}\left(1 - \frac{q^2}{m_b^2}\right)^2 \frac{q^2}{m_b^2}$$
$$\times (|C_S|^2 + |C'_S|^2). \quad (31)$$

When integrated between 1 and 6 GeV^2, this leads to a tiny correction,

$$\int_{1\,\mathrm{GeV}^2}^{6\,\mathrm{GeV}^2} \frac{d\mathrm{Br}(B \to X_s\mu^+\mu^-)}{dq^2} dq^2$$
$$= 1.59(17) \times 10^{-6}[1 + 0.007(1)(|C_S|^2 + |C'_S|^2)], \quad (32)$$

so that even the largest allowed values for $|C_S^{(l)}|$, displayed in Fig. 4, result in a negligibly small correction to the inclusive $B \to X_s\mu^+\mu^-$ rate.

(ii) We stress again that the NP scenario in which only the coupling to the scalar operators $\mathcal{O}^{(l)}$ are allowed would not modify the SM predictions of the q^2 shapes of three transverse asymmetries that can be measured from $B \to K^*\ell^+\ell^-$ decay, namely $A_T^{(2,\mathrm{im,re})}(q^2)$ [4].

B. $C_P^{(l)} \neq 0$

The situation is slightly more complicated in the case of $C_P \pm C'_P$ because both phases are needed. It is easy to see that Eq. (8) gives us

$$\left| C_P - C'_P + 2\frac{m_b m_\mu}{m_{B_s}^2} C_{10}^{\mathrm{SM}} \right|$$

$$\leq \frac{8\pi^{3/2} m_b}{\alpha G_F f_{B_s} m_{B_s}^2 |V_{tb}V_{ts}^*|}\sqrt{\frac{\mathrm{Br}(B_s \to \mu^+\mu^-)}{m_{B_s}\tau_{B_s}\beta_\mu(m_{B_s}^2)}} = 0.150,$$

(33)

and therefore considering only the relative phase, $\Delta\phi_P = \phi_{P'} - \phi_P$, is not enough. Instead, we write

$$|C_P|^2 + |C'_P|^2 - 2|C_P||C'_P|\cos(\Delta\phi_P) + \tilde{C}_{10}^2$$
$$+ 2\tilde{C}_{10}[|C_P|\cos\phi_P - |C'_P|\cos(\phi_P + \Delta\phi_P)] \leq (0.150)^2,$$
(34)

where, for brevity, we use $\tilde{C}_{10} = 2C_{10}^{\mathrm{SM}}m_b m_\mu/m_{B_s}^2$. Besides $\Delta\phi_P$, we choose to vary the phase of C_P. A compact analytical expression similar to Eq. (34) that constrains $C_P + C'_P$ from $\mathrm{Br}(B \to K\ell^+\ell^-)$ cannot be obtained. Instead, we get

$$|C_P + C'_P|_{m_\ell=0} \leq 1.3, \quad |C_P + C'_P - 0.33|_{m_\mu} \leq 1.3 \quad (1\sigma)$$
(35)

in the massless and massive lepton case, respectively. In what follows, we will use $m_\ell = m_\mu \neq 0$.

We first fix $\phi_P = 0$ and vary the relative phase $\Delta\phi_P \in [0, \pi]$. Typical examples are shown in Fig. 5. We then let
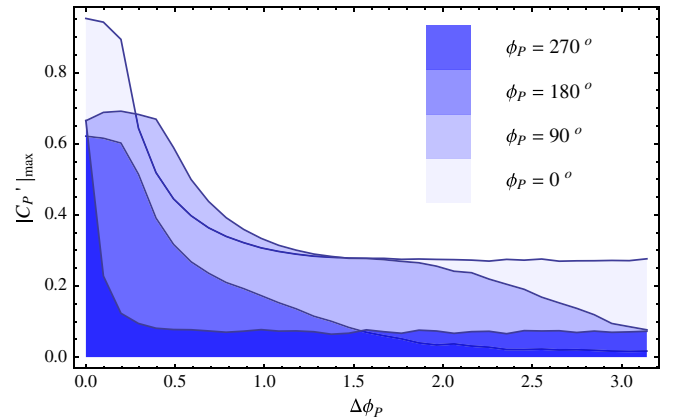

FIG. 6 (color online). Available values of $|C_P|$ or $|C'_P|$ allowed by the experimental results of Eqs. (9) and (21) are plotted as a function of the relative phase $\Delta\phi_P = \phi'_P - \phi_P$, for four different values of ϕ_P specified in the legend.
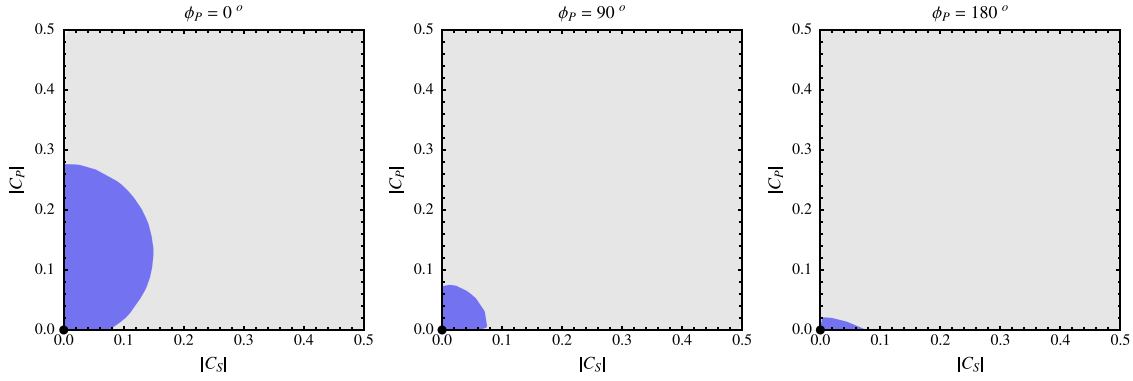
FIG. 7 (color online).   Allowed values for $|C_S|$ and $|C_P|$ obtained by combining the experimental information on $\mathrm{Br}(B \to K\ell^+\ell^-)$ (light shaded area) and the upper bound on $\mathrm{Br}(B_s \to \mu^+\mu^-)$ (dark shaded area). Illustration is provided for three various values of the relative phase ϕ_P.

$\phi_P \in (0, 2\pi]$ and observe that the possible values of $|C_P|$ and $|C_P'|$ consistent with Eqs. (9) and (21) are smaller than in the $\phi_P = 0$ case. For any fixed ϕ_P the situation is similar to what we observed in the case of $|C_S|$ and $|C_S'|$ (cf., Fig. 4), namely that for larger $\Delta\phi_P$ the possible values of $|C_P|$ and $|C_P'|$ are smaller than in the case $\Delta\phi_P = 0$. In other words, the most space available for NP occurs when the phases of $|C_P|$ and $|C_P'|$ are aligned ($\Delta\phi_P \approx 0$), and even more when the NP phase $\phi_P \approx 0$. This is illustrated in Fig. 6.

Furthermore, observations similar to those we made in the end of the previous subsection apply also in this case:

(i) Our result that $|C_P^{(\prime)}| \lesssim 1.0$ for any value of ϕ_P and for any $\Delta\phi_P$ is consistent with the observed branching fraction of the inclusive decay rate [Eq. (28)], which is modified by the presence of the pseudoscalar operator in the same way it was in the case of the scalars [29], namely,

$$\frac{d\mathrm{Br}(B \to X_s\mu^+\mu^-)}{dq^2}\bigg|_{C_P^{(\prime)}} = \frac{3B_0}{2m_b^2}\left(1 - \frac{q^2}{m_b^2}\right)^2 \frac{q^2}{m_b^2}$$
$$\times (|C_P|^2 + |C_P'|^2). \quad (36)$$

(ii) Notice also that the nonzero values of $C_P^{(\prime)} \neq 0$ cannot modify the SM predictions of the low q^2 shapes of three transverse asymmetries, $A_T^{(2,\mathrm{im,re})}$, currently studied in the $B \to K^*\ell^+\ell^-$ decay at LHCb.

C. Peculiar case of $C_{S,P} \neq 0$

Before closing this section, we would like to comment on the case, often discussed in the literature, in which the NP can couple via $C_{S,P} \neq 0$ but with $C_{S,P}' = 0$. The available range of values for $|C_{S,P}| \neq 0$ consistent with the constraints provided by $\mathrm{Br}(B \to K\ell^+\ell^-)$ and $\mathrm{Br}(B_s \to \mu^+\mu^-)$ is depicted in Fig. 7. As in the previous cases, the largest range of $|C_{S,P}| \neq 0$ is obtained when the pseudoscalar coupling is real, $\phi_P = 0$. The result is, of

course, invariant with respect to the change of the phase ϕ_S. A particularly important observation that can be made in this case is that the current constraint provided by $B \to K\ell^+\ell^-$ is redundant, but that situation could radically change if the errors on $B \to K$ form factors were significantly reduced. To illustrate that effect, we keep the central values of the form factors fixed and reduce the errors by 20%. In that hypothetical situation, the constraint coming from the measured and theoretically evaluated $\mathrm{Br}(B \to K\ell^+\ell^-)$ is not compatible with the SM (within the 1σ accuracy), and therefore $B \to K\ell^+\ell^-$ becomes an essential constraint to the values of possible $|C_{S,P}|$. The corresponding plots are presented in Fig. 8, where we only show the cases for which the overlapping region (satisfied by both constraints) exists. For $\phi_P \gtrsim 40°$ such a solution would not exist, which would be very valuable information about NP.

The above example only further highlights the importance of reducing the errors on the $B \to K$ transition form factors by using the currently available lattice QCD configurations that include $N_f = 2, 2 + 1$, and even $2 + 1 + 1$ dynamical quark flavors. We should also stress that simultaneous experimental effort in measuring the partial decay width of $B \to K\ell^+\ell^-$ at several moderately large and large values of q^2 would be highly welcome, because for those momentum transfers the uncertainties of the form factors computed in LQCD are under much better control than those at low q^2's. Effort in that direction made in Ref. [2] is highly welcome.

IV. CONSTRAINTS ON $C_{10}^{(\prime)}$

In this section we focus on the NP contributions that might arise from the couplings to the operator $\mathcal{O}_{10}$ and $\mathcal{O}_{10}'$, assuming that the Wilson coefficients $C_{S,P}^{(\prime)} = 0$, as in the SM.[3] Specific realizations of the two-Higgs

_____

[3]Here we also tacitly assume that the $C_{7,9,T}^{(\prime)}$, which enter the expression for $\mathrm{Br}(B \to K\ell^+\ell^-)$, remain at their SM values.
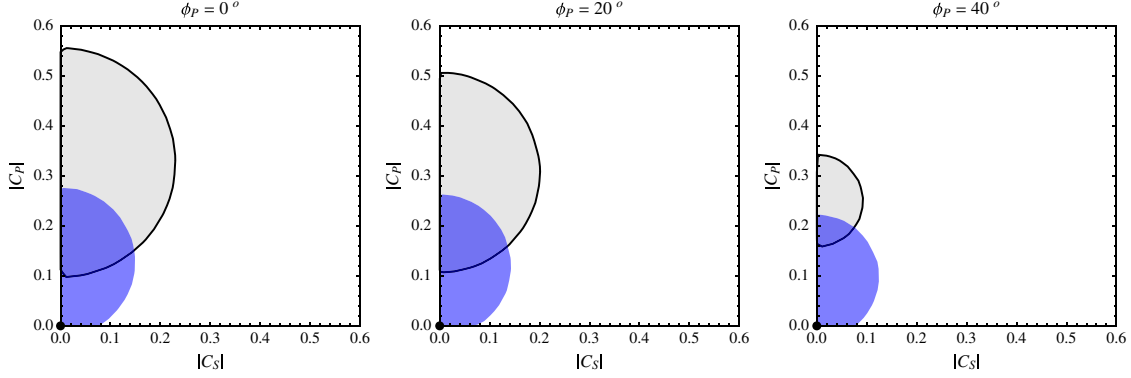
FIG. 8 (color online). Same as in Fig. 7, except that the errors on the hadronic form factors relevant to $B \to K\ell^+\ell^-$ are reduced by 20%, and we plot the cases with $\phi_P = 0$, 20° and 40°.

doublet models have been discussed in great detail in Refs. [22,30]. Note that our Wilson coefficients $C_{10}^{(I)}$ are related to the ones defined in Ref. [22] as

$$C_{10} = X(C_{LR}^V - C_{LL}^V)^*, \quad C_{10}' = X(C_{RR}^V - C_{RL}^V)^*, \quad (37)$$

where X is the same one defined after Eq. (25). From Refs. [22,30] we learn that

(i) The Z^0-penguin, with a charged Higgs running in the loop, gives rise to

$$
\begin{aligned}
C_{10}^{Z^0 H^+} &\propto +\frac{m_t^2}{m_W^2}\frac{1}{\tan^2\beta}, \\
C_{10}'^{Z^0 H^+} &\propto -\frac{m_s m_b}{m_W^2}\tan^2\beta.
\end{aligned}
\quad (38)
$$

Therefore, a nonzero contribution in the scenario is conceivable for either small or large $\tan\beta$, although the large $\tan\beta$ in C_{10}' is suppressed by the strange quark mass.

(ii) The Z^0-penguin, with a gluino running in the loop, is only relevant at larger $\tan\beta$, and the corresponding contributions are such that $C_{10}^{Z^0\tilde{g}} = C_{10}'^{Z^0\tilde{g}}$.

(iii) Box diagrams are highly suppressed and give no interesting contributions.

As far as the leptoquark models are concerned, C_{10} and C_{10}' can be nonzero in both classes of models, namely with scalar or vector leptoquarks. Interestingly, however, the change in $C_{10}^{(I)}$ implies the change in $C_9^{(I)}$ too. For more details about this issue, see Ref. [23].

In what follows, we proceed in a way similar to the previous section and use Eqs. (9) and (21) to obtain

$$|C_{10} + C_{10}'| \leq 4.4, \quad |C_{10} - C_{10}'| \leq 4.8 \quad (1\sigma). \quad (39)$$

It is now sufficient to study the impact of the relative phase, $\Delta\phi = \phi_{10'} - \phi_{10}$, by using

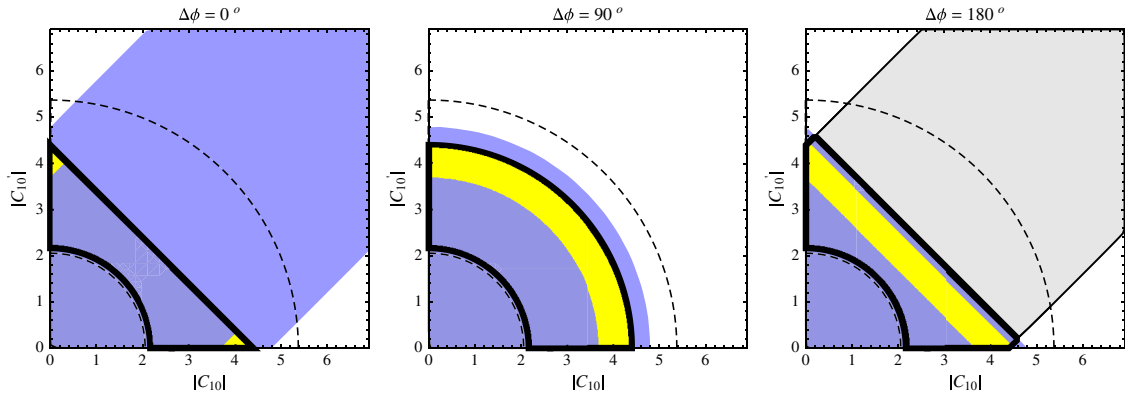$$|C_{10} \pm C_{10}'|^2 = |C_{10}|^2 + |C_{10}'|^2 \pm 2|C_{10}||C_{10}'|\cos(\Delta\phi). \quad (40)$$

FIG. 9 (color online). Constraint on $|C_{10}|$ and $|C_{10}'|$ obtained by combining the experimental information on $\mathrm{Br}(B \to K\ell^+\ell^-)$ (light shaded area) and $\mathrm{Br}(B_s \to \mu^+\mu^-)$ (dark shaded in the plots). We used the hadronic form factors and the decay constant given in Appendixes A and B. Three plots correspond to three specific choices of the relative phase $\Delta\phi = \phi_{10'} - \phi_{10}$ indicated in each plot. The domain inside the dashed curve is allowed by the inclusive decay, as indicated in Eq. (43). The region satisfying all three constraints is within the thick curve. See text for the explanation about the yellow region.

In Fig. 9 we illustrate the resulting constraints for three distinctive cases, $\Delta\phi = 0$, $\pi/2$, and π. We see that for $\Delta\phi = 0$ the main constraint comes from $B \to K\ell^+\ell^-$, whereas in the case of $\Delta\phi = \pi$ the decisive constraint is $B_s \to \mu^+\mu^-$, which is easy to understand from Eq. (40). In the intermediate case of $\Delta\phi = \pi/2$ the two constraints are equivalent.

We also checked the hypothetical scenario in which the measured $\mathrm{Br}(B_s \to \mu^+\mu^-)$ coincides with its value predicted in the SM [Eq. (9)]. As a result, the allowed region in the $|C_{10}|$-$|C'_{10}|$ plane is depicted by the yellow stripe in Fig. 9.

Contrary to the previous section, in this case the inclusive branching fraction [Eq. (28)] provides us with a valuable new constraint. The contribution from $\mathcal{O}_{10}^{(l)}$ to the differential decay rate can be extracted from Ref. [29], and for the massless lepton pair it reads

$$\frac{d\mathrm{Br}(B \to X_s\mu^+\mu^-)}{dq^2}\bigg|_{C_{10}^{(l)}} = \frac{B_0}{m_b^2}\left(1 - \frac{q^2}{m_b^2}\right)^2\left(1 + 2\frac{q^2}{m_b^2}\right)$$
$$\times (|C_{10}|^2 + |C'_{10}|^2), \quad (41)$$

and therefore we can write

$$10^6 \times \int_{1\,\mathrm{GeV}^2}^{6\,\mathrm{GeV}^2} \frac{d\mathrm{Br}(B \to X_s\mu^+\mu^-)}{dq^2} dq^2$$
$$= 0.69(9) + 0.058(6)(|C_{10}|^2 + |C'_{10}|^2). \quad (42)$$

When combined with the experimental value in Eq. (28), we get

$$4.7 \leq |C_{10}|^2 + |C'_{10}|^2 \leq 28.9 \quad (1\sigma). \quad (43)$$

As before, we account for the 1σ uncertainty around the central experimental value and take the lowest/largest possible values to obtain the limits in Eq. (43), which describes a disc in the $|C_{10}|$-$|C'_{10}|$ plane, as shown in Fig. 9 (dashed curves). The situation is now more interesting, as it depends considerably on the value of the relative phase. For $\Delta\phi = 0$, the constraint coming from $B \to K\ell^+\ell^-$ is overwhelming, and the one inferred from $B_s \to \mu^+\mu^-$ is only marginal. For $\Delta\phi = \pi$, the two constraints exchange roles, and the most stringent constraint comes from $B_s \to \mu^+\mu^-$. In the intermediate situation with $\Delta\phi = \pi/2$, the two constraints are equivalent and have shapes similar to that coming from $B \to X_s\mu^+\mu^-$. In Fig. 10 we show the possible values of $|C_{10}^{(l)}|$ compatible with all three constraints and for any $\Delta\phi \in [0, \pi]$.

Another difference with respect to the (pseudo)scalar operators discussed in the previous section is that the low q^2 dependence of the three transverse asymmetries, $A_T^{(2,\mathrm{im,re})}(q^2)$, extracted from the full angular analysis of $B \to K^*\ell^+\ell^-$ decay, are different from their SM shapes when the $C_{10}^{(l)}$ are modified by the NP contributions (see Ref. [4] for details). In particular, the
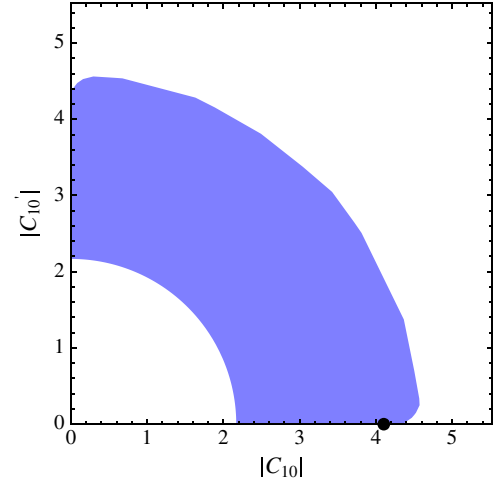

FIG. 10 (color online). The dark region describes the possible values of $|C_{10}|$ and $|C'_{10}|$ for any relative phase $\Delta\phi \in [0, \pi]$, obtained from the measured $\mathrm{Br}(B \to K\ell^+\ell^-)$, the upper bound on $\mathrm{Br}(B_s \to \mu^+\mu^-)$, and the branching fraction of the partial inclusive decay rate, cf., Eqs. (28) and (42). A thick dot corresponds to the Standard Model value, $C_{10} = -4.103$.

slope of the asymmetry $A_T^{(\mathrm{re})}(q^2)$ is highly sensitive to the value of C_{10},

$$\frac{\partial A_T^{(\mathrm{re})}(q^2)}{\partial q^2}\bigg|_{q^2=0} = R\frac{C_{10}}{2m_bC_7}, \quad (44)$$

where R is a convenient ratio of the $B \to K^*$ form factors.[4]

V. ON THE IMPORTANCE OF MEASURING THE FORWARD-BACKWARD ASYMMETRY IN $B \to K\ell^+\ell^-$ DECAY

The observation that the spectrum of $b \to s\ell^+\ell^-$ decays in the region of large $q^2 \gtrsim 15\,\mathrm{GeV}^2$ is not plagued by the $\bar{c}c$ resonances opened numerous possibilities for testing theory against experiment [31]. This is the region in which a major progress in taming the hadronic uncertainties by means of LQCD is possible, and therefore a more reliable extraction of physics BSM from experiment should be possible.

One quantity that we find particularly interesting to study at large q^2's is the forward-backward asymmetry $A_{FB}^\mu(q^2)$. In the SM this quantity is zero and remains as such, even if the NP considerably modifies the values of the Wilson coefficients $C_{7,9,10}^{(l)}$. On the other hand, if the NP gives rise to the new (non-SM) Dirac structures, $A_{FB}^\mu(q^2)$ can quite appreciably differ from zero. To our knowledge this observation was made for the first time in Ref. [32]. The expression for $A_{FB}^\mu(q^2)$ used in Ref. [32], however,

---

[4]More specifically, $R = (V/T_1)/(m_B + m_{K^*}) \approx (A_1/T_2)/(m_B - m_{K^*})$ [4].

differs from the one reported in Ref. [20]. We checked both formulas and agree with the one given in Ref. [20].

To get a better insight into the impact of NP on $A_{FB}^\ell(q^2)$, we expand it in powers of the lepton mass and write[5]

$$A_{FB}^\ell(q^2) = \frac{\mathcal{C}(q^2)}{\Gamma_\ell} \frac{m_B - m_K}{m_b} \sqrt{\lambda(q^2)} f_0(q^2)$$
$$\times \{2(C_S C_T + C_P C_{T5})q^2 f_T(q^2)$$
$$+ m_\ell[C_S C_9(m_B + m_K)f_+(q^2)$$
$$+ 2m_b(C_S C_7 + 2C_{T5}C_{10})f_T(q^2)]$$
$$+ \mathcal{O}(m_\ell^2)\}. \tag{45}$$

All the quantities in the above formula have already been defined in Sec. II B. Measuring $A_{FB}^\ell(q^2)$ at large q^2's would be highly beneficiary for our quest for NP at low energies. A separate experimental study of $A_{FB}^e(q^2)$ and $A_{FB}^\mu(q^2)$ would help us discern the first term from the second in Eq. (45). Notice that the first term is nonzero only if the NP coupling to a tensor operator is allowed. Therefore this quantity can be used to test the assumption we made in the previous sections of this paper when discussing $\mathrm{Br}(B \to K\ell^+\ell^-)$, namely that $C_{T,T5} = 0$, as in the SM.

Moreover, from the inclusive branching fraction [Eq. (28)] to which the tensor operators contribute as [29]

$$\frac{d\mathrm{Br}(B \to X_s\mu^+\mu^-)}{dq^2}\bigg|_{C_{T,T5}} = \frac{8B_0}{m_b^2}\left(1 - \frac{q^2}{m_b^2}\right)^2\left(2 + \frac{q^2}{m_b^2}\right)$$
$$\times (|C_T|^2 + |C_{T5}|^2), \tag{46}$$

one gets

$$\int_{1\,\mathrm{GeV}^2}^{6\,\mathrm{GeV}^2} \frac{d\mathrm{Br}(B \to X_s\mu^+\mu^-)}{dq^2} dq^2$$
$$= 1.59(17) \times 10^{-6}[1 + 0.66(9)(|C_T|^2 + |C_{T5}|^2)]. \tag{47}$$

Contrary to the (pseudo)scalar case in which the factor multiplying new Wilson coefficients is very small, cf., Eq. (32), the corresponding factor multiplying the tensor

---

[5]For simplicity, here we take the Wilson coefficients to be real. If they were all fully complex, then the expansion in Eq. (45) would look as follows:

$$A_{FB}^\ell(q^2) = \frac{\mathcal{C}(q^2)}{\Gamma_\ell} \frac{m_B - m_K}{m_b} \sqrt{\lambda(q^2)} f_0(q^2) \,\mathrm{Re}\{2[(C_S + C_S')C_T^*$$
$$+ (C_P + C_P')C_{T5}^*]q^2 f_T(q^2) + m_\ell[((C_S + C_S')$$
$$\times (C_9 + C_9')^*)(m_B + m_K)f_+(q^2) + 2m_b((C_S + C_S')$$
$$\times (C_7 + C_7')^*)f_T(q^2) + 2((C_{10} + C_{10}')C_{T5}^*)f_T(q^2)]$$
$$+ \mathcal{O}(m_\ell^2)\}.$$
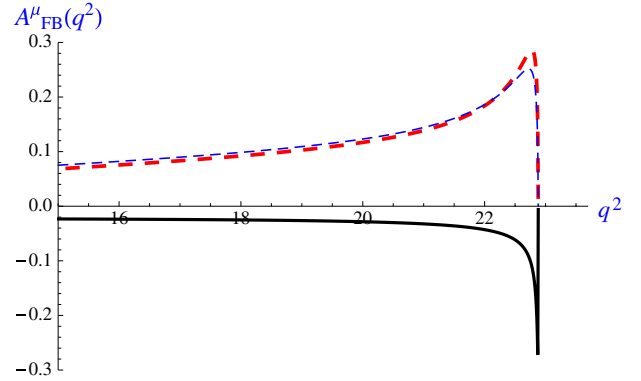

FIG. 11 (color online). Forward-backward asymmetry in $B \to K\mu^+\mu^-$ decay. The full curve is obtained with $C_T = C_{T5} = 1.1$ [consistent with Eq. (48)] and by keeping $C_{S,P} = 0$. The dashed curves, instead, are obtained with the same $C_T = C_{T5} = 1.1$, but with $C_S = 0$, $C_P = 1$ (thick dashed curve) or $C_P = 1$, $C_S = 0$ (thin dashed curve).

Wilson coefficients is much larger, and consequently the constraint provided by Eq. (28) is much stronger:

$$|C_T|^2 + |C_{T5}|^2 \lesssim 2.6. \tag{48}$$

For the sake of illustration, we take $C_T = C_{T5} = 1.1$ and plot $A_{FB}^\mu(q^2)$ in Fig. 11 at large q^2's by taking $C_{S,P} = 0$. With that choice, and due to the fact that we consider the decay to the pair of muons, the $A_{FB}^\mu(q^2) \neq 0$ everywhere and is strongly enhanced near $q_{max}^2 = (m_B - m_K)^2$. We then switch C_S or C_P to illustrate the case when the first term in Eq. (45) is nonzero. If indeed realized in nature, this latter situation would be relatively easy to check experimentally.

VI. SUMMARY

In this paper we showed that $B_s \to \mu^+\mu^-$ and $B \to K\ell^+\ell^-$, the two actively studied decays in the B physics experiments, provide us with complementary information about potential NP contributions. While the decay amplitude for $B_s \to \mu^+\mu^-$ is proportional to the difference between the Wilson coefficients of the operators of opposite chirality, the $B \to K\ell^+\ell^-$ involves the sum of these Wilson coefficients.

We checked the situations in which the NP enters either via the scalar, the pseudoscalar, or the semileptonic operators. To decide which situation is verified in nature (if any), useful information can be obtained from the low-q^2 shapes of the transverse asymmetries in $B \to K^*\ell^+\ell^-$ decay. Those asymmetries are being studied in experiments and have an important advantage in that the relevant hadronic uncertainties are small. A nonzero coupling to the scalar and/or pseudoscalar operator would not modify the low-q^2 shapes of these asymmetries. From $B_s \to \mu^+\mu^-$ and $B \to K\ell^+\ell^-$ we find the absolute bounds

$$|C_S^{(\prime)}| \lesssim 0.7, \qquad |C_P^{(\prime)}| \lesssim 1.0, \tag{49}$$

that are valid for any value of the NP phases. In fact, the values for $|C_{S,P}^{(l)}|$ can be considerably reduced if the non-zero NP phases are allowed.

In the case in which the coupling to the semileptonic operators $\mathcal{O}_{10}'$ is modified by the presence of NP particles, the transverse asymmetries in $B \to K^* \ell^+ \ell^-$ would have peculiar shapes, different from those predicted in the SM. From our study of $B_s \to \mu^+ \mu^-$ and $B \to K \ell^+ \ell^-$ we obtain that

$$2.2 \lesssim \sqrt{|C_{10}|^2 + |C_{10}'|^2} \lesssim 4.8, \tag{50}$$

regardless of the value of the relative NP phase. Note that the lower bound is fixed by the experimentally measured partial decay rate of the inclusive $B \to X_s \mu^+ \mu^-$ decay.

In considering $B \to K \ell^+ \ell^-$ we ignored the contributions from the tensor operators. That assumption can also be experimentally tested by measuring the nonzero forward-backward asymmetry in $B \to K \ell^+ \ell^-$ decay.

Our approach of considering a pair of Wilson coefficients at a time is orthogonal to the global fit approach adopted in many recent works. We have checked explicitly our results with the results of Bobeth *et al.* in Ref. [19], where a fit to real Wilson coefficients $C_{7,9,10}$ also included the experimental observables related to $B \to K^* \ell^+ \ell^-$ and $B \to K^* \gamma$. Our results in the scenario with complex C_{10} and C_{10}' (Fig. 10) agree well with their presented range of real C_{10}. We have also checked our allowed regions for Wilson coefficients against the results of the global fit presented in Altmannshofer *et al.* in Ref. [19].

In this paper we focused either on the quantities that have small hadronic uncertainties, or those for which the hadronic uncertainties are likely to be improved soon. This is particularly the case with the $B \to K$ form factors, that we computed in the quenched approximation of QCD, which will soon be improved by including the effect of light dynamical quarks. Detailed experimental information about the partial decay rate of $B \to K \ell^+ \ell^-$ in the upper range of q^2's will become particularly useful, because the results for the form factors computed on the lattice at larger q^2's are more reliable and have smaller errors.

Note added.—While this paper was in writing, the new results for Br$(B \to K \ell^+ \ell^-)$, measured at LHCb, appeared in Ref. [38]. Their value is lower than the one reported by *BABAR* [2], and the agreement with the current theoretical estimate of the same quantity is only at the 2σ level. Once a more reliable estimate of the $B \to K$ form factors computed on the lattice becomes available, we will repeat the analysis presented here by including the 1, 2, 3σ effects.

APPENDIX A: $B \to K$ FORM FACTORS

The results for the form factors used in this paper are obtained from the analysis following the same procedure as the one explained in detail in Ref. [33], but by using the (quenched) gauge field configurations obtained at finer lattice spacing [$a^{-1} = 3.8(1)$ GeV]. Those configurations have been used to compute the $B \to K^* \gamma$ form factors in Ref. [34], and we refer the reader to that paper for lattice details.

Besides the form factors $f_+(q^2)$ and $f_0(q^2)$ computed along the lines explained in Ref. [33], we also computed the tensor form factor $f_T(q^2)$ appearing in Eq. (16). Note that the tensor density depends on the renormalization scale that we have set to $\mu = m_b$, the same scale at which the corresponding Wilson coefficients have been computed.

It is easy to extend the parameterization of Ref. [35] to include the form factor $f_T(q^2)$ and keep the minimal number of parameters needed to describe the q^2 dependence of all three form factors. In terms of poles exchanged in the t-channel, the q^2 dependence of $f_T(q^2; \mu)$ is driven by the states with $J^P = 1^-$.[6] The lowest such a state is B_s^*, whose couplings to the vector and tensor bilinear quark operators are defined via

$$\langle 0|\bar{s}\gamma_\mu b|B^*(p, \varepsilon_r)\rangle = \varepsilon_\mu^{*r} m_{B^*} f_{B_s^*}^V,$$
$$\langle 0|\bar{s}\sigma_{\mu\nu} b|B^*(p, \varepsilon_r)\rangle = i(p_\mu \varepsilon_\nu^{*r} - p_\nu \varepsilon_\mu^{*r}) f_{B_s^*}^T(\mu). \tag{A1}$$

The nearest pole contribution then reads

$$\langle K(k)|\bar{s}\gamma_\mu b|B(p)\rangle^{\text{pole}} = \sum_r \frac{\langle 0|\bar{s}\gamma_\mu b|B_s^*(q, \varepsilon_r)\rangle\langle B_s^*(\varepsilon_r)|BK\rangle}{q^2 - m_{B_s^*}^2}$$
$$= -\frac{1}{2}\left(p^\mu + k^\mu - \frac{m_B^2 - m_K^2}{q^2} q^\mu\right)$$
$$\times \frac{m_{B_s^*} f_{B_s^*}^V g_{B_s^* BK}}{q^2 - m_{B_s^*}^2},$$
$$\Rightarrow f_+^{\text{pole}}(q^2) = \frac{-\frac{1}{2} m_{B_s^*} f_{B_s^*}^V g_{B_s^* BK}}{q^2 - m_{B_s^*}^2}, \tag{A2}$$

where we used the standard definition $\langle B_s^*(\varepsilon_r)|BK\rangle = g_{B_s^* BK}(k \cdot \varepsilon_r)$. Similarly, for the matrix element of the

---

[6]Notice in particular that couplings to 1^+ states are ruled out when both external states are pseudoscalars.

tensor quark operator we have

$$\langle K(p_K)|\bar{s}\sigma_{\mu\nu}b|B(p_B)\rangle^{\text{pole}}$$

$$= \sum_r \frac{\langle 0|\bar{s}\sigma_{\mu\nu}b|B_s^*(q,\varepsilon_r)\rangle\langle B_s^*(\varepsilon_r)|BK\rangle}{q^2 - m_{B_s^*}^2}$$

$$\Rightarrow f_T^{\text{pole}}(q^2;\mu) = \frac{-\frac{1}{2}(m_B + m_K)f_{B_s^*}^T(\mu)g_{B_s^*BK}}{q^2 - m_{B_s^*}^2}, \quad \text{(A3)}$$

and therefore the residua of these two form factors are related, i.e.,

$$\text{Res}_{q^2 \to m_{B_s^*}^2} f_T(q^2;\mu) = \frac{m_B + m_K}{m_{B_s^*}} \frac{f_{B_s^*}^T(\mu)}{f_{B_s^*}^V} \text{Res}_{q^2 \to m_{B_s^*}^2} f_+(q^2).$$

$$\text{(A4)}$$

It is quite remarkable to note that the pole dominance, that is expected to be reasonable at large q^2's (small recoils), leads to a simple proportionality relation between $f_T(q^2)$ and $f_+(q^2)$, namely

$$\frac{f_T(q^2;\mu)}{f_+(q^2)} = \frac{m_B + m_K}{m_{B_s^*}} \frac{f_{B_s^*}^T(\mu)}{f_{B_s^*}^V}, \quad \text{(A5)}$$

which is essentially verified in the low-q^2 region (large recoils), as obtained in Ref. [36,37]:

TABLE I. $B \to K\ell^+\ell^-$ form factors at several values of q^2. The renormalization scale for the tensor form factor is $\mu = m_b$.

$q^2[\text{GeV}^2]$	$f_0(q^2)$	$f_+(q^2)$	$f_T(q^2)$
13.0	0.51(6)	0.90(9)	0.80(11)
14.5	0.54(6)	1.04(9)	0.92(12)
15.9	0.57(7)	1.21(11)	1.07(14)
17.4	0.61(7)	1.45(13)	1.27(17)
18.8	0.65(7)	1.75(18)	1.52(20)
20.3	0.70(8)	2.19(22)	1.89(21)

$$\frac{f_T(q^2)}{f_+(q^2)} \approx \frac{m_B + m_K}{m_B}. \quad \text{(A6)}$$

On the basis of Eq. (A4), it is judicious to define the scale independent

$$\tilde{f}_T(q^2) = \frac{m_{B_s^*}}{m_B + m_K} \frac{f_{B_s^*}^V}{f_{B_s^*}^T(\mu)} f_T(q^2;\mu), \quad \text{(A7)}$$

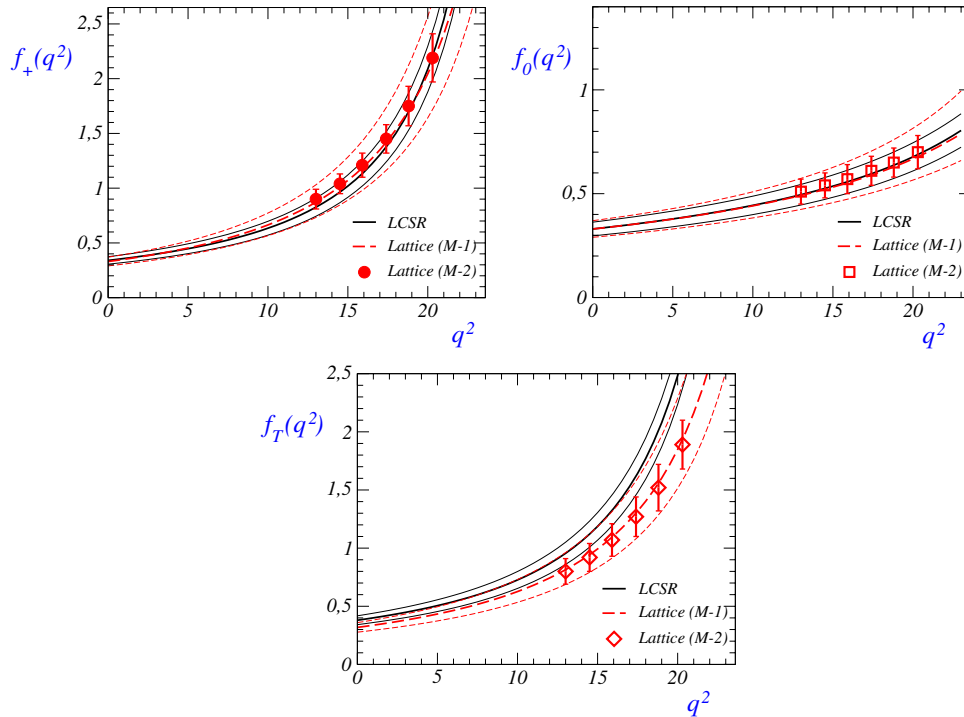which then can be easily included in the parameterization of Ref. [35] as

FIG. 12 (color online). Comparison of the q^2 dependence of the $B \to K$ transition form factors as obtained in quenched lattice QCD with the predictions based on using the QCD sum rules near the light cone.

TABLE II.   All the scale-dependent quantities are obtained in the $\overline{\text{MS}}$ renormalization scheme. The Wilson coefficients are evaluated at the next-to-next-to leading logarithms. $\alpha_s(M_Z) = 0.118$.

$C_7^{\text{eff}}(m_b)$	-0.304	[9,10]	m_μ	0.10566 GeV	[14]
$C_9^{\text{eff}}(m_b)$	4.211	[9,10]	$m_b(m_b)$	4.25(12) GeV	[14]
$C_{10}^{\text{eff}}(m_b)$	-4.103	[9,10]	m_K	0.495 GeV	[14]
τ_{B_s}	1.47 ps	[14]	m_B	5.279 GeV	[14]
τ_{B^0}	1.52(1) ps	[14]	m_{B_s}	5.366(1) GeV	[14]
$\alpha \equiv \alpha_{\text{em}}(M_Z^2)$	1/128.94(3)	[15]	f_{B_s}	0.234(10) GeV	[16,17]
G_F	1.1664×10^{-5} GeV^{-2}	[14]	$|V_{tb}V_{ts}^*|$	0.0403(8)	[18]

$$f_0(q^2) = \frac{c(1-\alpha)}{1 - q^2/(\beta m_{B_s^*}^2)},$$

$$f_+(q^2) = \frac{c(1-\alpha)}{(1 - q^2/m_{B_s^*}^2)(1 - \alpha q^2/m_{B_s^*}^2)}, \qquad \text{(A8)}$$

$$\tilde{f}_T(q^2) = \frac{c(1-\alpha_T)}{(1 - q^2/m_{B_s^*}^2)(1 - \alpha_T q^2/m_{B_s^*}^2)},$$

so that only one new parameter (α_T) is needed to fit all three form factors. The values of form factors extracted at various q^2 from our lattice computation are listed in Table I, where we also used $f_{B_s^*}^T(m_b)/f_{B_s^*} = 0.91(3)$, computed on the same lattices. In terms of the above parameters, we have

$$f_+(0) = f_0(0) = 0.33(4), \quad \tilde{f}_T(0) = 0.31(4)$$
$$\alpha = 0.72(14), \quad \alpha_T = 0.67(15), \quad \beta = 1.35(15), \quad \text{(A9)}$$

which are obtained either by extrapolating the parameters to the B-meson mass (M-1), or by fitting the results from Table I (M-2) to the parameterization in Eq. (A8).

We should stress that the results for the form factors presented and used in this paper are obtained in the quenched approximation of QCD, and that they will be updated very soon by using the available gauge field configurations in which the effects of the light sea quarks have been included. We also note that the results for the

form factors presented here are compatible with those obtained by using the LCSR, which are parameterized as follows [6]:

$$f_0(q^2) = \frac{0.331(4)}{1 - q^2/6.12^2},$$

$$f_+(q^2) = \frac{0.162(21)}{1 - q^2/5.41^2} + \frac{0.173(22)}{(1 - q^2/5.41^2)^2}, \qquad \text{(A10)}$$

$$f_T(q^2) = \frac{0.161(21)}{1 - q^2/5.41^2} + \frac{0.198(25)}{(1 - q^2/5.41^2)^2},$$

and illustrated in Fig. 12.

APPENDIX B: NUMERICAL VALUES OF THE QUANTITIES USED IN THIS WORK

The values of all quantities used in this work are listed in Table II. Two comments are in order.

(i) We use $\tau_B = \tau_{B^0}$ to respect the experimental practice when combining the charged and neutral $\text{Br}(B \to K\ell^+\ell^-)$ decay modes.

(ii) Taking the continuum results of three unquenched simulations from Ref. [16] in the quadrature, one gets the average $f_{B_s} = 0.234(6)$ GeV, which is marginally compatible with a spectacularly accurate result reported in Ref. [17]. We inflated the error to include the central value of Ref. [17].

[1] R. Ammar *et al.* (CLEO Collaboration), Phys. Rev. Lett. **71**, 674 (1993).

[2] J. P. Lees *et al.* (BABAR Collaboration), arXiv:1204.3933.

[3] R. Aaij *et al.* (LHCb Collaboration), Phys. Rev. Lett. **108**, 231801 (2012).

[4] D. Becirevic and E. Schneider, Nucl. Phys. **B854**, 321 (2012).

[5] D. Melikhov, N. Nikitin, and S. Simula, Phys. Lett. B **442**, 381 (1998); F. Kruger and J. Matias, Phys. Rev. D **71**, 094009 (2005).

[6] P. Ball and R. Zwicky, Phys. Rev. D **71**, 014029 (2005); A. Khodjamirian, T. Mannel, and N. Offen, Phys. Rev. D **75**, 054013 (2007).

[7] R. Zhou *et al.* (Fermilab Lattice and MILC Collaborations), Proc. Sci., LATTICE2011 (2011) 298 [arXiv:1111.0981]; D. Becirevic *et al.* (unpublished).

[8] B. Grinstein, M. J. Savage, and M. B. Wise, Nucl. Phys. **B319**, 271 (1989); M. Misiak, Nucl. Phys. **B393**, 23 (1993); **B439**, 461(E) (1995); A. J. Buras and M. Munz, Phys. Rev. D **52**, 186 (1995).

[9] C. Bobeth, M. Misiak, and J. Urban, Nucl. Phys. **B574,** 291 (2000).

[10] W. Altmannshofer, P. Ball, A. Bharucha, A. J. Buras, D. M. Straub, and M. Wick, J. High Energy Phys. 01 (2009) 019.

[11] A. J. Buras, M. Misiak, M. Münz, and S. Pokorski, Nucl. Phys. **B424,** 374 (1994).

[12] K. De Bruyn, R. Fleischer, R. Knegjens, P. Koppenburg, M. Merk, A. Pellegrino, and N. Tuning, Phys. Rev. Lett. **109,** 041801 (2012).

[13] R. Aaij *et al.* (LHCb Collaboration), Phys. Rev. Lett. **108,** 101803 (2012); **108,** 241801 (2012).

[14] K. Nakamura *et al.* (Particle Data Group), J. Phys. G **37,** 075021 (2010).

[15] A. D. Martin, J. Outhwaite, and M. G. Ryskin, Eur. Phys. J. C **19,** 681 (2001).

[16] A. Bazavov *et al.* (Fermilab Lattice and MILC Collaboration), Phys. Rev. D **85,** 114506 (2012); H. Na, C. J. Monahan, C. T. H. Davies, R. Horgan, G. P. Lepage, and J. Shigemitsu, arXiv:1202.4914; P. Dimopoulos *et al.* (ETM Collaboration), J. High Energy Phys. 01 (2012) 046.

[17] C. McNeile, C. T. H. Davies, E. Follana, K. Hornbostel, and G. P. Lepage, Phys. Rev. D **85,** 031503 (2012).

[18] J. Charles, O. Deschamps, S. Descotes-Genon, R. Itoh, H. Lacker, A. Menzel, S. Monteil, V. Niess *et al.*, Phys. Rev. D **84,** 033005 (2011); M. Bona, A. J. Bevan, M. Ciuchini, D. Derkach, E. Franco, L. Silvestrini, V. Lubicz, C. Tarantino *et al.*, Proc. Sci., FPCP2010 (2010) 039.

[19] A. J. Buras and J. Girrbach, arXiv:1204.5064; F. Mahmoudi, S. Neshatpour, and J. Orloff, arXiv:1205.1845; F. Beaujean, C. Bobeth, D. van Dyk, and C. Wacker, arXiv:1205.1838; W. Altmannshofer, P. Paradisi, and D. M. Straub, J. High Energy Phys. 04 (2012) 008; S. Descotes-Genon, D. Ghosh, J. Matias, and M. Ramon, J. High Energy Phys. 06 (2011) 099; J. Matias, F. Mescia, M. Ramon, and J. Virto, J. High Energy Phys. 04 (2012) 104; J. Drobnak, S. Fajfer, and J. F. Kamenik, Nucl. Phys. **B855,** 82 (2012); K. de Bruyn, R. Fleischer, R. Knegjens, P. Koppenburg, M. Merk, A. Pellegrino, and N. Tuning, Phys. Rev. Lett. **109,** 041801 (2012); A. Behring, C. Gross, G. Hiller, and S. Schacht, arXiv:1205.1500; D. Ghosh, M. Guchait, S. Raychaudhuri, and D. Sengupta, arXiv:1205.2283 [Phys. Rev. D (to be published)]; A. K. Alok, A. Datta, A. Dighe, M. Duraisamy, D. Ghosh, and D. London, J. High Energy Phys. 11 (2011) 121.

[20] C. Bobeth, G. Hiller, and G. Piranishvili, J. High Energy Phys. 12 (2007) 040.

[21] A. Abada, D. Becirevic, P. Boucaud, J. M. Flynn, J. P. Leroy, V. Lubicz, and F. Mescia (SPQcdR Collaboration), Nucl. Phys. B, Proc. Suppl. **119,** 625 (2003); K. C. Bowler, J. F. Gill, C. M. Maynard, and J. M. Flynn (UKQCD Collaboration), J. High Energy Phys. 05 (2004) 035.

[22] P. H. Chankowski and L. Slawianowska, Phys. Rev. D **63,** 054012 (2001); G. Isidori and A. Retico, J. High Energy Phys. 11 (2001) 001.

[23] N. Kosnik, arXiv:1206.2970.

[24] M. Iwasaki *et al.* (Belle Collaboration), Phys. Rev. D **72,** 092005 (2005).

[25] B. Aubert *et al.* (*BABAR* Collaboration), Phys. Rev. Lett. **93,** 081802 (2004).

[26] T. Huber, T. Hurth, and E. Lunghi, Nucl. Phys. **B802,** 40 (2008).

[27] A. Ali, E. Lunghi, C. Greub, and G. Hiller, Phys. Rev. D **66,** 034002 (2002).

[28] K. G. Chetyrkin and M. Steinhauser, Nucl. Phys. **B573,** 617 (2000).

[29] S. Fukae, C. S. Kim, T. Morozumi, and T. Yoshikawa, Phys. Rev. D **59,** 074013 (1999).

[30] H. E. Logan and U. Nierste, Nucl. Phys. **B586,** 39 (2000).

[31] C. Bobeth, G. Hiller, D. van Dyk, and C. Wacker, J. High Energy Phys. 01 (2012) 107; M. Beylich, G. Buchalla, and T. Feldmann, Eur. Phys. J. C **71,** 1635 (2011); M. Bartsch, M. Beylich, G. Buchalla, and D.-N. Gao, J. High Energy Phys. 11 (2009) 011.

[32] A. K. Alok, A. Dighe, and S. U. Sankar, Phys. Rev. D **78,** 114025 (2008).

[33] A. Abada, D. Becirevic, P. Boucaud, J. P. Leroy, V. Lubicz, and F. Mescia, Nucl. Phys. **B619,** 565 (2001).

[34] D. Becirevic, V. Lubicz, and F. Mescia, Nucl. Phys. **B769,** 31 (2007).

[35] D. Becirevic and A. B. Kaidalov, Phys. Lett. B **478,** 417 (2000).

[36] J. Charles, A. Le Yaouanc, L. Oliver, O. Pene, and J. C. Raynal, Phys. Rev. D **60,** 014001 (1999).

[37] M. Beneke, A. P. Chapovsky, M. Diehl, and T. Feldmann, Nucl. Phys. **B643,** 431 (2002); D. Pirjol and I. W. Stewart, Phys. Rev. D **67,** 094005 (2003); **69,** 019903 (2004).

[38] R. Aaij *et al.* (LHCb Collaboration), J. High Energy Phys. 07 (2012) 133.